Journal of ELECTRICAL ENGINEERING, VOL. 52, NO. 5-6, 2001, 125–133

EFFECTS OF SOLAR IRRADIATION CONDITIONS AND OTHER FACTORS ON THE OUTDOOR PERFORMANCE OF PHOTOVOLTAIC MODULES

Hamdy K. Elminir [*] — **Vítězslav Benda** [*] — **Jiří Toušek** [**]

The operating efficiency of an installed photovoltaic module is not well predicted by its datasheet, related to standard test conditions: normal and unpolarized light, 1000 W/m^2 of irradiance, AM1.5 spectrum and 25 °C of cell temperature. These reference conditions in fact are hardly attainable in the field as they combine the irradiance of a clear summer day with the module temperature of a clear winter day and spectrum of a clear spring day. Thus, the energy supplied by the module in the field can be 30 % lower than expected. From this point of view, it is of great importance to reveal the characteristics of photovoltaic modules in actual use conditions for a long-term period. This long-term investigation of photovoltaic modules, however, will give more reliable information about their practical performance than indoor measurement as the modules experience seasonal changes all the year. This study illustrates a comprehensive experimental study of the effects of environmental factors on both the efficiency and electrical power output of photovoltaic modules. Atmospheric conditions, angle of incidence, solar position, orientation of the cell, and cell temperature are considered as the key environmental parameters in this study.

K e y w o r d s: Solar irradiation conditions; Angle of incidence; Orientation of the cell; Dust deposition density; Linke turbidity factor; Ångström turbidity coefficient.

1 INTRODUCTION

During the last few years, there has been an increasing interest in the natural degradation processes that occur on solar collectors mounted outdoors. Many freshly installed modules already show a reduction in their electric (or thermal) performance after a few weeks of operation. Since the losses continuously increase in the course of time, collector efficiency may drop to very low values after only a few years; hence the study of the natural degradation of photovoltaic cells is of particular importance.

There have been several studies that analyze uncertainties in laboratory measurement of solar cell efficiencies using different solar simulators and their transference to operational situations ([20 23]). Gonzalez et al. (1994) examines variation of modeled and observed cell efficiencies with atmospheric variations. The major factors found to cause variations in operation efficiency are ambient air temperature and total irradiance intensity. The authors also observed increases of the apparent efficiency of amorphous cells, decreasing energy in the red portion of the solar spectrum, which are consistent with model predictions. Hirata Y. and Tani T. [13, 14] developed a method to calculate the output of photovoltaic modules with allowance for the effects of spectral solar radiation variation. These calculated values were then compared with measured values. The results confirmed that the output of photovoltaic modules changes seasonally in proportion to changes in spectral solar radiation. This provided strong evidence that seasonal variation in spectral solar radiation should be taken into account for optimum design. Hirata et al. [15] investigated more specifically how seasonal changes in cell temperature and spectral solar radiation affect the variation in conversion efficiency for CdS-CdTe and two-layers tandem-amorphous silicon, 2L a- Si. The following points were clarified:

- The mean monthly cell temperature ranged between 14 and 40 °C while that for 2L a-Si varied from 21 to 48 °C. The available spectral ratio had a seasonal variation of 9 % for CdS-CdTe and a substantially higher 16 % for 2L a-Si.
- The relative conversion efficiency of CdS-CdTe increased during summer by 7 %, whereas 2L a-Si exhibited a more substantial 14 % variation.

The increase in terrestrial applications of solar radiant energy has given impetus to the study of solar energy availability in many areas of the world. With the increasing use of spectrally selective devices, such as photovoltaic cells for electrical generation and selective absorbers for thermal collectors, and for practical applications in environmental and agrometeorological research, current interest is not only in the total amount of solar energy reaching the Earth's surface but also in its spectral composition. Atmospheric pollutants and aerosols play an important role in regulating the amount of solar radiation absorbed by the Earth-atmosphere system. In one of the earliest studies, Garg, H.P. [10] found that the normal transmittance of direct solar radiation of glass or plastic sheets at

[*] Czech Technical University, Faculty of Electrical Engineering, Technická 2, 166 27 Praha 6, Czech Republic, ehamdy@hotmail.com
[**] Charles University, Faculty of Mathematics and Physics, Ke Karlovu 3, 121 16 Praha 2, Czech Republic

ISSN 1335-3632

different angles of tilt reduced from 90 % to about 45 % at an angle of 15° after 30 days of exposure and reduced by an average of 8 % for glass tilted at 45° after 30 days of exposure. Information about the dust pollution level and dust particles during the test period was not given. Said, S. [26] has shown the degradation rate of the efficiency for a photovoltaic panel due to sand dust accumulation on the panel at Dhahran, Saudi Arabia. The photovoltaic panel tests were conducted at solar noontime when the current and voltage values were measured ranging from open circuit to short circuit limits. The panel was oriented to the south facing with a tilt angle of 26°. The results for the test period indicated a continuous decrease in the efficiency ratio with a minimum of less than 40 % of the initial clean panel value. The decrease in the efficiency ratio was about 11 % per month, while it was 7 % in second year tests due to more rainfall and fewer sand dust storms at the same location. El-Shobokshy, M. S. and Hussein, F. M. [9] indicate that the nature of the dust, such as the dust material, its size distribution and the dust deposition density has a strong influence on the loss of output from the solar cells.

Orientation and tilt angle of a photovoltaic modules and solar collector are the two most important factors usually considered in solar energy system design. One of the methods for increasing the efficiency of the solar energy system is to use the optimum orientation and tilt angle. There have been several interesting articles that appeared in the previous decade to predict the optimum orientation and tilt angle. Some simple rules were specified for the collector tilt angle, relative only to the latitude [5, 12, 16, 27]. Chiou, J. P. and El-Naggar, M. M. [6] presented an analytical method to determine the optimum tilt angle of a plate facing the equator only in the heating season. They finally concluded that the optimum tilt angle in the heating season is about $\phi + (10 \rightarrow 30°)$. Baloukts et al. [3] studied the tilt angle and photovoltaic energy for four locations Gavods (35° N), Kythons (37.42° N) in Greece, Bet Degan (31° N) in Israel and Portiand (45.6° N) in USA. They employed two methods for estimating the optimum tilt angle and setting its seasonal variation, which depend on the clearness index. In this paper, we report the results of evaluation of both a-Si: H and poly-Si modules, which were carried out for one year at outdoor conditions. Two parameters were used to examine the performance of both types of PV module: the efficiency and electrical output power. From these evaluations we get information as to how to achieve the operating efficiency and integrated output power of a-Si: H and poly-Si module close to their standard test conditions values.

Table 1. Filter characteristics

Old name	Filter Reference	Interval Bands (μm)	Filter Factor f
OG1	OG530	0.530–0.630	1.082
RG2	RG630	0.630–0.695	1.068
RG8	RG695	0.695–2.900	1.042

2 LOCATION OF STUDY

The photovoltaic modules and measuring apparatus were installed on the terrace of the research laboratory in the National Research Institute of Astronomy and Geophysics, Helwan, Egypt (29.87° N, 31.33° E rise from M.S.L. about 124 m). A very common weather condition in the city of Helwan is characterized by calm or light air, increased humidity during the cold season. The daily average of temperature in Helwan ranges between 35.2 °C in July and 13.1 °C in January. The relative humidity fluctuates between 39 % in June and 56 % in December, and visibility about 5 km. This restricted visibility is the result of the presence of solid particles in the atmosphere some of which act as condensation nuclei. During such a weather condition, the reduction of solar radiation is sometimes due to the increased quantity of water vapor, sometimes to the presence of increased quantities of aerosol particles and sometimes to the presence of both these influences. The major sources of pollution at Helwan are due to three types of factories:

- Cement factories, which include four factories distributed from the north in Tura to the south in El-Tebeen
- Engineering industries (cars factory, pipes and tubes factory)
- Iron and steel factories

The major source of wind direction is from the N and N-E, which represents about 50 % of the total direction. This means that Tura El-Cement and Helwan Cement factories represent 50 % of the pollution of Helwan region. The National Cement factory and Iran and Steel factories represent about 40 % of the total pollution of the Helwan region.

3 MEASUREMENT APPARATUS

In this study, the broadband filter method was used to measure the quantities of normal radiation at different bands. The Schott filters, OG1, RG2, and RG8, were arranged on a rotatable disk and mounted on Eppley Normal Incidence Pyrheliometer. The measured intensity through the filters was normally used to compute turbidity with the methods described by Linke [19] and Ångström [2]. The transmission bands of the filters used in these measurements are in Tab. 1

Total radiation on the plane of the PV modules was monitored with a high precision pyranometer, which is sensitive in the wavelength range from 300 to 3000 nm. Sky diffuse radiation was measured by a pyranometer equipped with a special shading device to exclude direct radiation from the sun. Meteorological instrumentation was used to provide the necessary information about the

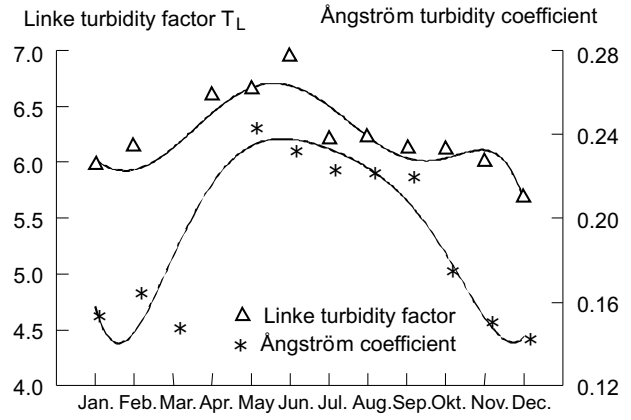

Fig. 1. Annual evolution of monthly mean values for T_L, and β

weather. These data were used to determine the stability class of the atmosphere from which the rate of dust deposition was calculated. The concentration of dust in the atmosphere was monitored by means of a portable air sampler. The physical design of this sampler is based on aerodynamic principles, which results in the collection of particles of 100 microns and less. For measuring the concentration, air was drawn into the sampler, and, by virtue of their inertia, the particles were deposited on membrane filters. The filters were weighted before and after sampling to determine the mass collected. The weight was divided by the surface area from which they were collected to give the dust deposition density in $\mathrm{g/m^2}$. Two commercially available photovoltaic panels were tested during the measurements. The first panel was a flat plate solar panel containing three squared amorphous silicon solar cells $30 \times 30\,\mathrm{cm}^2$ with $\eta = 6.91\,\%$ produced by Chronar, UK. The second panel was a polycrystalline solar cell as a panel (3 modules) $37.5\,\mathrm{cm}^2$ with $\eta = 14.45\,\%$ produced by (PJ2), Japan. Cell temperatures were measured using a thermocouple, which was laminated on the back surface of the PV modules using a conductive paste to ensure good thermal contact.

4 DESCRIPTION AND DEFINITION OF SOLAR DATA

All data sets were subjected to various quality control tests. Three types of data checks were performed to identify missing data, data, which clearly violate physical limits, and extreme data. Hours when the data were known to be "bad" or "missing" were omitted. Second, any hour with an observation that violated a physical limit or conservation principle was eliminated from the data set, including: reported hours with diffuse fraction greater than 1, or beam radiation exceeding the extraterrestrial beam radiation. To eliminate the uncertainty associated with radiation measurements at large incidence angles, hours with a zenith angle larger than 80° were eliminated. The final data set was constructed from the measured data that passed all of the quality control checks.

5 MATHEMATICAL FORMULATION

The reduction of solar radiation is a very important parameter when it refers to areas of increased atmospheric pollution such as big cities and industrial areas. The most interesting information is the fact that the atmosphere cannot clean itself when a specific limit of pollution has been reached [25].

5.1. Determination of the Different Atmospheric Turbidity Parameter

Among the atmospheric turbidity coefficients, which have been described in literature, the most frequently used are the Linke turbidity factor, T_L, and Ångström turbidity coefficient, β. Linke's turbidity factor is an index of the number of clear dry atmospheres that would be necessary to produce the attenuation of the extraterrestrial radiation that is produced by the real atmosphere. The Linke turbidity factor is estimated from the expression

$$T_L = P(m)\big(\log G_o - \log G - 2\log R\big) \tag{1}$$

where, $P(m)$ is a function of the optical air mass, m. The values of $P(m)$ which are used in this study are obtained by the next empirical formula which is the best fit of the values given by Coulson [7]:

$$P(m) = 22.64\,\mathrm{m}^{-0.801} \quad \text{for } 1 \le m \le 4\,. \tag{2}$$

The relative optical air mass, m, of the average atmosphere was computed from equation, corrected for pressure variations [17]:

$$m = \left[\cos\theta_Z + 0.50572(96.07995 - \theta_Z)^{-1.6364}\right]^{-1}. \tag{3}$$

The Ångström turbidity coefficient, β, was computed using the direct solar radiation for spectral range (0.250–0.695μm) and a constant value of $\alpha = 1.3$. The computation of the Ångström turbidity coefficient, β, was made from the relation

$$d_{A\lambda} = \beta\lambda^{-\alpha}\,. \tag{4}$$

Figure 1 presents the annual evolution of the monthly mean values for the Linke turbidity factor, T_L, and Ångström turbidity coefficient, β, during the measurement period. All of them show similar evolutions, with the higher values in the summer and lower values in winter. This result is in good agreement with many other studies [1, 22] that mention pronounced maximum in summer and minimum in winter. We note that autumn and spring values are rather high and closer to summer values than to winter values. The variations of atmospheric turbidity coefficients indicate that the atmosphere in Helwan city is mostly turbid throughout the year.

Table 2. Optimum tilt angles at Helwan

Month	Jan	Feb	Mar	Apr	May	Jun	Jul	Aug	Sep	Oct	Nov	Dec
K_T	0.23	0.26	0.29	0.28	0.31	0.40	0.35	0.37	0.31	0.32	0.29	0.25
N	15	47	74	105	135	166	196	227	258	288	319	349
ρ	0.2	0.2	0.2	0.2	0.2	0.2	0.2	0.2	0.2	0.2	0.2	0.2
$\beta_{\text{Opt.}}$	43°	36°	27°	16°	7°	2°	4°	12°	24°	35°	43°	45°

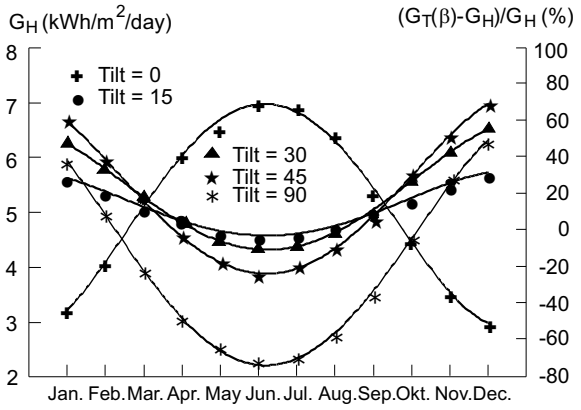

Fig. 2. Annual cycle of: long-term monthly average global solar radiation received by horizontal surface, "+", (left axis); long term average percent deviations of daily global solar irradiation received by tilted south oriented surface from a horizontal surface at the same site (right axis)

5.2 Determination of Solar Radiation on Tilted South Oriented Surfaces

Quantitative assessment of solar radiation incident on a tilt plane is very important to engineers designing solar energy collecting devices, to architects designing buildings, and to agronomists studying insolation on vegetation on mountain slopes. To meet all these requirements, one should know the intensity of radiation falling upon the sloping surface and its variation over a period of one year. The equations describing the instantaneous total insolation on a tilted surface, under the assumption of anisotropic distribution of the diffuse sky was presented in the following form, [18]:

$$G_T = (G_H - I_{d,H})\cdot R_b + I_{d,H}\Big[\frac{1+\cos\beta_T}{2}\Big(1+F_1\sin^3\frac{\beta_T}{2}\Big) \times \big(1+F_1\cos^2\theta_i\sin^3\theta_Z\big)\Big] + \frac{1}{2}G_H\rho\big(1-\cos\beta_T\big) \quad (5)$$

$$R_b = \frac{\cos\theta_i}{\cos\theta_Z} = \frac{\sin\delta\sin(\phi-\beta_T)+\cos\delta\cos\omega\cos(\phi-\beta_T)}{\cos\phi\cos\delta\cos\omega+\sin\phi\sin\delta} \quad (6)$$

$$F_1 = 1-\Big(\frac{I_{d,H}}{G_H}\Big)^2. \quad (7)$$

The percentage deviations of the long-term monthly average global irradiations received by tilted surfaces compared with that received by a horizontal surface are shown in Fig. 2. This figure underlines the fact: an inclined, south oriented pyranometer obtains more global solar radiation during winter than a horizontal pyranometer does in northern mid latitudes. The excess is largest if the tilt angle of the pyranometer equals the geographical latitude of the station. During summer the excess is nearly $-5\,\%$ for $\beta_T \le 30°$ but it becomes more and more negative with increasing tilt angle.

5.3 Choice of The Angle of Tilt For South Facing Solar Collectors

The method outlined in the previous section for estimating the average radiation on surfaces of various orientations can be used to show the effects of slope and azimuth angle on the total energy received on a surface on a monthly, seasonal, or annual basis. From the previous review, and according to Elsayed, M.M., 1989, one can show that the optimum tilt angle depends on several parameters as indicated below:

$$\beta_{\text{Opt.}} = \big(6-4.8\,K_T+0.86\,{K_T}^{0.27}\,\phi+0.0021\phi^2\big) + \big(31\,{K_T}^{0.37}+0.094\,{K_T}^{0.46}\,\phi+0.000634\,{K_T}^{-0.17}\,\phi^2\big) \times\cos\Big[\frac{360}{365}(N+11.5)\Big] \quad (8)$$

Depending on the application, it is usually required for the applications of the flat plate collectors to determine one optimum tilt angle for a given season. Using the previous results, the seasonal optimum tilt angle is estimated using the following relation:

$$\beta_{\text{Opt.}} = \frac{\sum_{K=i}^{j}\beta_{\text{Opt},K}\cdot G_{H,K}}{\sum_{K=i}^{j}G_{H,K}} \quad (9)$$

where, i and j refer to the order of the beginning and ending month of the season and K refers to any month within the season. For yearly optimum tilt, Equation 9 can also be applied using $i = 1$ and $j = 12$. Using the previous formula, the predicted optimum tilt angle for each month at Helwan is tabulated in Table 2.

Using the data measured at Helwan, together with the correlations given by eqns (8) and (9) the yearly optimum tilt is found equal to 21°.

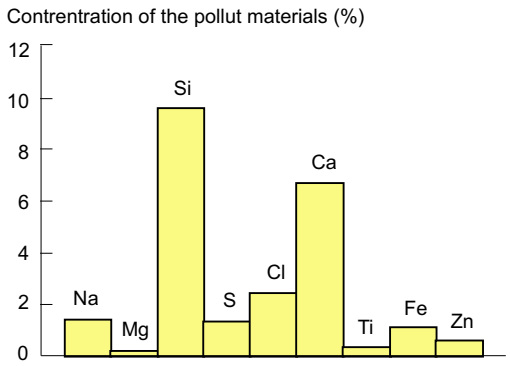

Fig. 3. Results of X-ray fluorescent analysis of dust particles

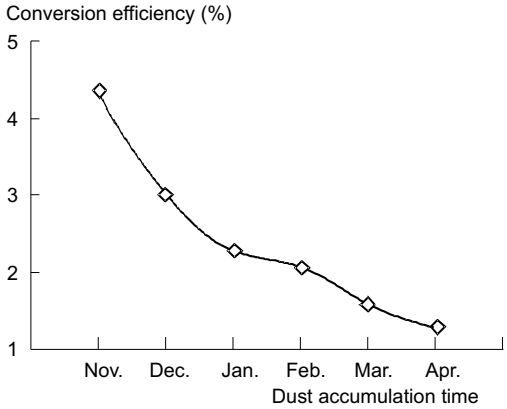

Fig. 4. The depression of the efficiency after six months due to sand-dust accumulation on a-Si:H

Table 3. Annual mean value of G, TSP and Smoke for Cairo and Helwan

Region	G_H (kWh/m^2/day)	TSP (μg/m^3)	Smoke (μg/m^3)
Cairo	5.03	583	132
Helwan	5.48	960	52

6 EXPERIMENTAL RESULTS AND DISCUSSIONS

The potential for photovoltaic solar energy applications in Egypt is enormous. This is true since this country possesses practically all the basic ingredients required for productive utilization of PV solar energy. That is, great number of sunshine hours $>$ 3000 hours per year), high solar radiation intensity (6 kWh/m^2/day as annual and regional average), and a very few cloudy days per year. The deposition of dust and particulates matter still, however, remains a major problem facing the photovoltaic systems. The rate of decrease in the efficiency depends mainly on the rate of dust deposition. The latter is a strong function of the dust concentration in the atmosphere. Therefore, the investigation of the effect of dust on the efficiency of PV cells necessitates the monitoring of dust concentration in the atmosphere around the module and its variation with time.

6.1 Solar Radiation Reduction by Aerosols in the area of Helwan

In the visible band (0.4–0.75μm), where gaseous absorption is minimal under clear sky conditions, aerosols are the major cause of depletion of direct beam solar radiation through scattering and absorption. There are two dominant layers of aerosols in the atmosphere — one near the Earth's surface (0–3 km), which is affected by natural dust storms and man-made inputs to the atmosphere, and another stratospheric dust layer (15–25 km above sea level) affected by volcanic action and cosmic sources. Regarding to the global solar radiation data for Cairo and Helwan, it is found that Helwan annual mean value was 5.48 kWh/m^2/day, which is higher than Cairo one which was 5.03 kWh/m^2/day, while the total suspended particles, TSP annual mean value for Helwan was 960 μg/m^3 and it was 583 μg/m^3 for Cairo. Also, the smoke annual mean value for Helwan was 52 μg/m^3, while it was 132 μg/m^3 for Cairo as shown in Tab. 3, [21].

From Tab. 3, it is found that the global solar radiation value for Helwan is higher than it is for Cairo by 8.2 %, TSP value for Helwan is higher than its for Cairo by 55 % and the smoke value for Cairo is higher than for Helwan by 61 %. Also, it is found that the increasing in global solar radiation ratio for Helwan than Cairo is due to the presence of higher value of TSP, which contains elements have large sizes like sand, calcium and iron, see Fig. 3. The presence of these elements leads to diffusion of the beam solar radiation to become diffuse solar radiation which is added to global solar radiation value and substitute the reduction in it due to the reduction in the direct solar radiation while the major element in Cairo is the smoke which makes absorption stronger than diffusion for the beam solar radiation. This makes a reduction to the global solar radiation value.

As could be expected, heavily polluted air (high dust concentrations) leads, in a same time interval, to larger degradation in power output from cells than less polluted air (small dust concentrations). High dust concentrations lead to high accumulation values on the cell surface. Figure 4 shows the change in the conversion efficiency as a function of dust accumulation. The results imply that the depression of the efficiency η is 33.5 % after one month and increases to 65.8 % after six months later without panel cleaning. At the end of the test period, the panel was cleaned and tested. The ratio of this clean test efficiency to the original clean test efficiency was 0.98, indicating that the degradation in performance was due to the dust and not a change in the panel cells themselves.

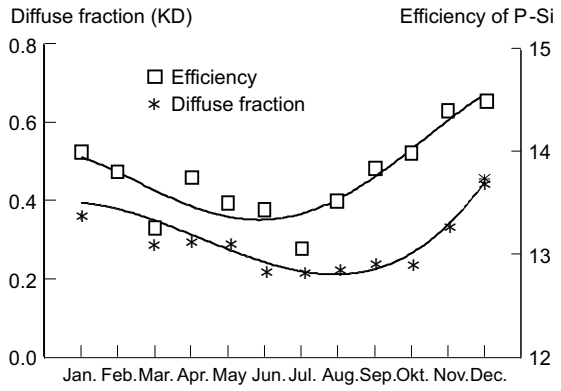

Fig. 5. Mean monthly variation of diffuse ratio and efficiency of P-Si module

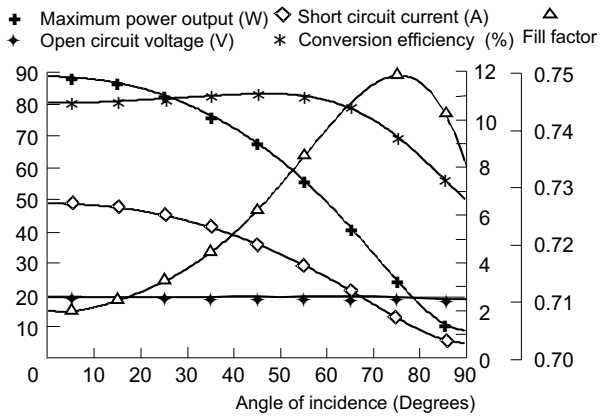

Fig. 6. AOI Functions showing influence of solar angle of incidence on Cell parameters

6.2 Performance Variation Of PV Cells Under Cloudy Skies

It is quite evident that local weather — mostly in the form of cloud cover — has an impact on the received radiation. The clouds not only block the reception of beam radiation but they also subtract from or add to the diffuse component depending on their albedo. The angular distributions of the diffuse radiance from partially cloudy skies, and skies containing multiple layers of clouds, are both complex and random, [24]. The cloudiness is greater in Lower Egypt than in Upper Egypt and reaches its maximum in winter while its minimum value is attained in summer. On many days at early morning low strut forms, especially over places in the Nile delta and Cannel zone. These formation is due to less radiation and turbulence in the humidity and usually disperses within two to four hours after sunrise, leaving, generally a clear sky until the following morning.

When the sky is cloudy, the amount of sunlight that is readily convertible into electricity by photovoltaic cell is reduced by at least 50 % during thin cirrus cloud cover and by about 75 % more during denser cloud cover. At any time of the day, the conditions of the atmosphere can be expressed quantitatively by the diffuse fraction, K_D (defined as the ratio of intensity of diffuse radiation to intensity of global or total radiation). K_D is lower under clear atmospheric conditions and high under turbid or cloudy atmosphere. The values of K_D lie between zero and unity, depending on atmospheric condition, K_D approaches unity under heavily overcast conditions. The optimum efficiency of a solar cell or array of cells will therefore vary with diffuse fraction as seen in Fig. 5.

6.3 Influence of Solar Angle –of- Incidence

Photovoltaic modules have an Angle-Of-Incidence, (AOI) dependent optical behavior that can be measured and used to improve the analysis of array performance. Like absolute air mass, solar angle of incidence is time of day dependent. Its affect on the short circuit current of a PV module results from two causes. The first is familiar to solar enthusiasts as the "cosine effect". The "cosine effect" is independent of the module design, and is only geometry related. Due to the cosine effect, the short circuit current from a module varies directly with the cosine of the AOI. For example, at $\mathrm{AOI} = 60°$ the cosine effect reduces the short circuit current by one half compared to the normal incidence condition.

The second way in which the short circuit current is affected by the AOI is dependent on the module design. The optical characteristics of the module materials located between the sun and the solar cells cause the effect. For all modules, light enters an optical compound made of cover glass, encapsulant, antireflecting coating of cell and/or cell texturisation, to be finally absorbed in the cells. While reflection and efficiency of modules are optimized for perpendicular incidence at standard test conditions, outdoor irradiance spans a much wider range of incidence angles. Above 40° incidence angle the reflectivity starts to increase and reaches 20 % losses at 75°. The influence of a module's optical characteristics on its performance can also be measured under outdoor test conditions in a straightforward manner. The measurement procedure developed provided an empirical function $F(\mathrm{AOI})$ that related the module's parameters to the solar angle of incidence. The AOI-Function addresses the effects that are beyond the typical geometric "cosine" losses. David L. et al. [8] give the method used for calculating $F(\mathrm{AOI})$.

$$\mathrm{AOI} = \cos^{-1}\left[\cos\beta \cdot \cos\theta_Z + \sin\beta \cdot \sin\theta_Z \cdot \cos(\alpha - \gamma)\right] \tag{11}$$

$$F(\mathrm{AOI}) = \frac{I_{SC}\left(\mathrm{AM}\,1.5, \mathrm{T} = 25°\right) - C_2 I_{d,H}/1000}{C_1 \cdot (I_{dni}/1000) \cdot \cos(\mathrm{AOI})} \tag{12}$$

Figure 6 shows the measured AOI-Functions for a typical flat-plate PV module with a glass front surface.

6.4 On the Choice of the Angle of Tilt for South Facing PV Module

Whereas the previous section described the direct impact of the operating conditions on module power, some

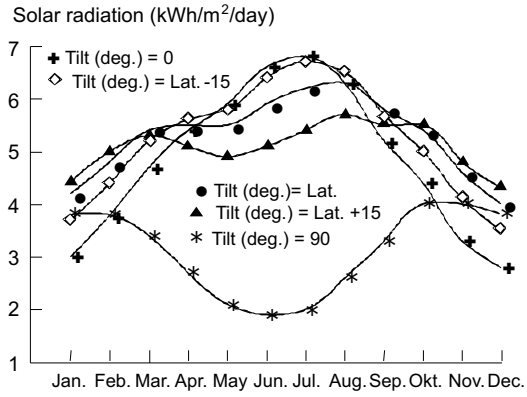

Fig. 7. Annual variation in estimating average daily radiation for flat plate collector facing south

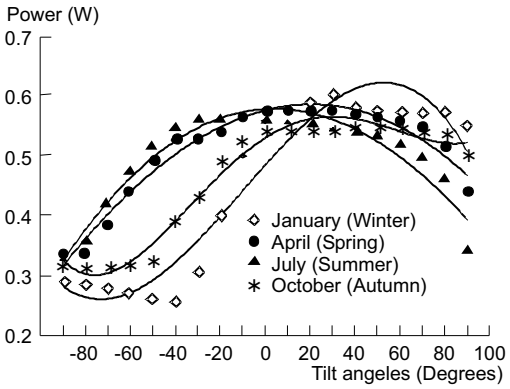

Fig. 8. Performance of a-Si:H module at different tilt angles

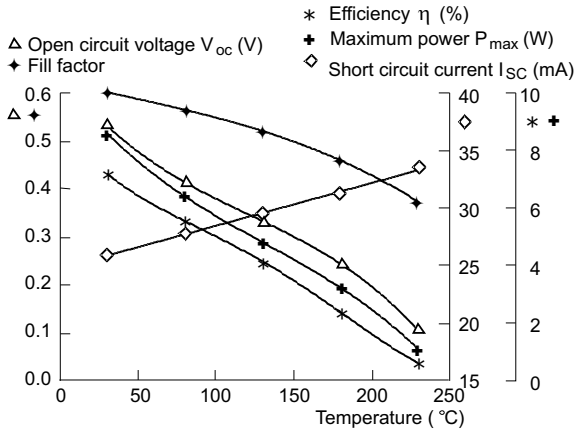

Fig. 9. Variation of key parameters of silicon solar cell at high temperatures

of these losses are a function of the installation properties, additionally. Reflection losses, for example, are governed by the incidence angle of the irradiation, but this can be influenced by the orientation of the module. Also the light levels are a function of incidence angle and module tilt. Due to the lack of measured tilted surface solar radiation data, models are employed to estimate the radiation incident on a collector surface from measured horizontal radiation. The results of these calculations are plotted against the angle of tilt for summer, winter and all year round intended use. To illustrate the effects of the receiving surface slope on monthly average daily radiation, the methods of section 5.2 have been used to estimate G_T for surfaces of several slopes, for values of $\phi = 29.87°$, $\gamma = 0°$, and ground reflectance $\rho = 0.2$. Figure 7 shows the variations of G_T through the year and shows the marked differences in energy received by surfaces of various slopes in summer and winter and indicates that there is one angle of tilt that offers maximum solar radiation interception to the south facing inclined surface of a flat plate collector. The optimum angle of tilt of a photovoltaic panel for use during the heating season months of November, December, January, February and March is approximately $45°$, to optimize performance in the summer, the collector can be tilted at $15°$. As seen from the previous paragraph, the optimum tilt angle of solar radiation collection systems located in Helwan follows the general rule applied by many researchers that during the heating season solar collectors should be given a tilt of Lat. $+15°$. Figure 8 shows the smooth fitting of the measurements for selective days in four months. Each month represents a season, (January for winter, April for spring, July for summer, and October for autumn). The tests were started when the PV module is vertical and north facing, the test continues to the horizontal mode, and completed to south facing with tilt angle $+90°$. Every ten degrees variation in the tilt angle, the module parameters (current, Voltage, and electrical output power) were recorded. Figure 8 shows that our experimental results seem to agree quite well with the predicted values of using Elsayed M.M., (1989) [see section 3.2].

6.5 The Effect of Cell Temperature

The daytime temperature of a solar cell is not simply equal to the ambient temperature, since solar cells are dark in color and therefore absorb a greater portion of the sun's energy. During the day, a solar cell operates hotter than the ambient temperature by a factor that depends on insulation. As the cell temperature increases, the short circuit current, I_{SC} somewhat increases, and the maximum power, $P_{\max}$, the efficiency, η, open circuit voltage, V_{oc}, and the fill factor, $F.F$ decrease as shown in Fig. 9.

The short circuit current increase with temperature is attributed to light absorption variation. Under the conditions considered, the solar absorption edge shifts due to a decrease of the crystal forbidden gap width and the number of pairs generated in the bulk increases. Alternatively, as the temperature increases, the intrinsic light absorption factor changes and the short circuit current increases. In the investigated specimens, the temperature coefficient of the short circuit current is approximately $\Delta I_{SC}/\Delta T = +40\mu\text{A}/\,°\text{C}$.

To explain the variation of the V_{oc} with temperature the effects of all voltage controlling parameters (mobility,

lifetime, energy band gap and absorption coefficient) have to be included in the analysis. In the general case, the open circuit voltage is determined by the relation $V_{OC} \approx \ln(I_{SC}/I_O)$, by which V_{oc} must grow as I_{SC} increases. Depending on the current flow mechanism, the value of I_o is proportional to n_i^2. As the temperature increases n_i grows exponentially and causes an exponential growth of I_o. Moreover, the crystal forbidden gap narrowing with temperature increase leads to the dark current increase and minimizes the positive effect of absorption factor. As a result, V_{OC} decreases in $\Delta V_{OC}/\Delta T = -2.3\,\mathrm{mV/\,°C}$.

The maximum power across the optimal load and the efficiency depend strongly on temperature; the shape of this dependence is close to linear. The temperature power coefficient and efficiency are about $-0.4\,\mathrm{mW/\,°C}$ and $-0.4\,\%/\,°\mathrm{C}$, respectively.

6.6 Effect of Humidity on PV Modules

The moisture content of the atmosphere is commonly expressed by relative humidity, defined as the ratio of actual water vapor pressure contained in the air to the saturated water vapor pressure at the same temperature. Air with a constant water vapor content will lead to a decrease in relative humidity with a rise in temperature. Water vapor in the atmosphere is invisible to human eye, but is "seen" by solar cells. The primary effect of humidity on terrestrial solar cells is corrosion, especially in the simultaneous presence of high temperature. The most corrosive phenomenon on a solar cell array is the potential deterioration of the titanium-silver contact on silicon solar cells in humid environments. Conditions of high temperature ($> 40\,°\mathrm{C}$) and humidity ($> 60\,\%$) can cause long-term deterioration of these contacts. Typically, higher temperatures and higher humidity levels accelerate the corrosion process, as may be the presence of minute quantities of ionization contaminate (such as salts). Other effects include a growth of fungi, the growth rates are the highest at relative humidity levels between 75 % and 95 % and at temperatures between 20 °C and 40 °C and the formation of a sticky surface film of moisture that catches dust and dirt particles. It has been proven that the conversion efficiency of PV modules drops progressively as dust is accumulated on its surface [See section (6.1)].

7 SUMMARY AND CONCLUSIONS

Most environments have a detrimental effect on the long-term performance capability of solar cell arrays. The most significant environments against which terrestrial array must be protected include high wind, snow and ice loading and corrosion aided by high temperature, moisture, and air borne contaminants. Beneficial environments for terrestrial array include low air temperature and moderate wind velocities that increase the solar cell operating efficiency.

Dust accumulation on transparent surfaces of PV-modules has a damaging effect on their transmittance and the reduction in transmittance depends on the quantity of the settled dust. Also, it may be concluded from this study that the effect of dust on the performance of photovoltaic solar cells can longer be correlated to the dust concentration in the atmosphere around the module.

As can be seen, the maximum tilt angles are required during the winter months and they drop sharply towards the summer months. Between April and September a near horizontal surface will obtain the maximum daily insolation. The monthly optimum tilt angles are given in Table 2. To optimize performance in the winter, the collector can be tilted 15° greater than the latitude angle; to optimize performance in summer, the collector can tilted 15° less than the latitude angle.

8 NOMENCLATURE

G	The intensity of solar radiation on the ground, $\mathrm{W/m^2}$
G_o	The intensity of solar radiation at the limit of the atmosphere, $\mathrm{W/m^2}$
G_H	Hourly global radiation incident on a horizontal surface, $\mathrm{kWh/m^2}$
G_T	Hourly global radiation incident on an inclined surface, $\mathrm{kWh/m^2}$
I_{dni}	The direct normal radiation
$I_{b,T}$	Hourly beam radiation incident on an inclined surface $\mathrm{kWh/m^2}$
$I_{d,H}$	Hourly sky diffuse radiation incident on a horizontal surface, $\mathrm{kWh/m^2}$
K_T	The monthly average clearness index
K_D	The diffuse fraction
M	Optical air mass
R	The Earth-Sun distance in astronomical units
ϕ	Latitude, degrees
δ	Declination, degrees
θ_Z	The zenith angle, degrees
θ_i	Incidence angle, the angle between beam radiation and the vertical, degrees
α	Azimuth angle of the Sun, degrees
γ	Azimuth angle of the PV-module (0° = North, 90° = East)
ω	Sunrise hour angle, degrees
β_T	Surface slope, degrees
β_{Opt}	Optimum tilt angle, degrees
ρ	Ground albedo
$d_{A\lambda}$	The aerosol optical depth and is dimensionless
λ	The wavelength, μm
α	Is a function of concentration and size distribution of particles

C_1, C_2 Calibration constants for direct and diffuse irradiance, respectively

N Number of the day on the year ($1 \rightarrow 365$), 1 January is No. 1

T_a Ambient air temperature, °C

T_c Solar cell Temperature under no wind, °C

K Solar cell temperature coefficient

I_o The diode reverse saturation current

References

[1] ABDEL-RAHMAN, M. A.—SAID, S. A.—SHUAIB, A. N.: Comparison Between Atmospheric Turbidity Coefficients of Desert and Temperate Climates, Solar Energy **40** (1988), 219.

[2] ÅNGSTRÖM, A.: Techniques of Determining the Turbidity of the Atmosphere, Tellus **13** (1961), 214.

[3] BALOUKTS, A.—TSANAKAS, D.—VACHTSEVANAS, G.: On the Optimum Tilt Angle of PV Array, Solar Energy **5** (1987), 155.

[4] BOUAOUADJA, N.—BOUZID, S.—HAMIDOUCHE, M.—BOUSBA, C.: Effects of the Sandblasting on the Efficiencies of Solar Panels, Applied Energy **65** (2000), 99.

[5] CHINNERY, D. W.: Solar Water Heating in South Africa, CSIR-Research report 248, 1971.

[6] CHIOU, J. P.—EL-NAGGAR, M. M.: Optimum Slop for Solar Insolation on a Tilted Surface without a Singularity at Zero Azimuth, Solar Energy **28** (1986), 357.

[7] COULSON, K. L.: Solar and Terrestrial Radiation, Academic Press, New York, 1975.

[8] DAVID, L. K.—JAY, A. K.—WILLIAM, E. B.: Measuring Solar Spectral and Angle of Incidence Effects on Photovoltaic Modules and Solar Irradiance Sensors, Presented at the 26$^{\text{th}}$ IEEE Photovoltaic Specialists Conference, California, 1997.

[9] EL-SHOBOKSHY, M. S—HUSSEIN, F. M.: Effect of Dust with Different Physical Properties on the Performance of Photovoltaic Cells, Solar Energy **51** (1993), 505.

[10] GARG, H. P.: Effect of Dirt on Transparent Covers in Flat Plate Solar Energy Collectors, Solar Energy **15** (1974), 299.

[11] GRASSI, G.: Two Year Experience of the EC Photovoltaic Pilot Projects, In: Proceeding 18$^{\text{th}}$ IEEE Photovoltaic Specialists Conference, Las Vegas, 1985, p. 871.

[12] HEY, H.: Operating Experience with Solar Water Heating, JIHVE **39** (1971), 63.

[13] HIRATA, Y.—TANI, T.: Evaluation of Photovoltaic Modules Considered Spectral Solar Radiation, Electrical Engineering in Japan, Scripta Technica **114** No. 8 (1994).

[14] HIRATA, Y.—TANI, T.: Output Variations of Photovoltaic Modules with Environmental Factors — I. The Effect of Spectral Solar Radiation on Photovoltaic Module Output, Solar Energy **55** No. 6 (1995), 463.

[15] HIRATA, Y.—INASAKA, T.—TANI, T.: Output Variations of Photovoltaic Modules with Environmental Factors — II. Seasonal Variation, Solar Energy **63** (1998), 185.

[16] HOTTEL, H. C.: Performance of Flat Plate Solar Energy Collectors. Space Heating with Solar Energy, Proc. of a Course-Symp., M.I.T Press, Cambridge, 1954.

[17] KASTEN, F.—YOUNG, A. T.: Revised Optical Air Mass Tables and Approximation Formula, Applied Optics **28** (1989), 4735.

[18] KLUCHER, T. M.: Evaluation of Models to Predict Insolation on Tilted Surfaces, Solar Energy **23** (1979), 114.

[19] LINKE, F.: Transmission Koeffizient und Trubungsfaktor, Beitr. Phys. Atoms **10** (1922).

[20] MATSON, R. J.—EMERY, K. A.—BIRD, R. E.: Terrestrial Solar Spectra, Solar Simulation and Solar Cell Short Circuit Current Calibration, Solar Cells **11** (1984), 105.

[21] MOSALAM, M. A.—ABDEL-HADY, K.—ABDEL-AZIZ, A.—HASSAN, A. H.—FATHY, A. M.: Atmospheric Turbidity over Menia, The 2$^{\text{nd}}$ Symposium and Exhibition on Renewable Energy and Modern Technologies for Environment Protection (AREEP), Ismailia, Egypt, 1998.

[22] MOSALAM, M. A.—TADROS, M. T.—EL-METWALLY, M.: Studying the Extinction Coefficient Due to Aerosol Particles at Different Spectral Bands in Some Regions at Great Cairo, Renewable Energy **19** (2000), 597.

[23] OSTERWALD, C. R.: Translation of Device Performance Measurements to Reference Conditions, Solar Cells **18** (1986), 269.

[24] ROSEN, M.: The Characterization and Modeling of the Angular Distribution of Diffuse Sky Radiance, M.Sc. Thesis, Dept. of Mechanical Engineering, Univ. of Toronto, 1983.

[25] SAHSAMANOGLOU, H.—BLOUTSOS, A.: Cleansing of the Atmosphere in the Athens Area by Means of Rainfall and Wind, The Impact of Climate Planning and Building, Elsevier, 1982, 125.

[26] SAID, S.: Effect of Dust Accumulation on Performances of Thermal and PV Flat Plate Collectors, Applied Energy **37** (1990), 73.

[27] YELLOT, J. I.: Utilization of Sun and Sky Radiation for Heating and Cooling of Buildings, ASHRAE J. **15** No. 12 (1973), 31.

Received 22 January 2001

Hamdy Kamal Elminir was born in EI_Mahala, Egypt in 1968. He received the BSc in Engineering, from Monofia university Egypt in 1991 and completed master degree in automatic control system, Mansoura university, Egypt in 1996. Currently he is a postgraduate student in the Department of Electrotechnology at Czech Technical University in Prague, Faculty of Electrical Engineering.

Vítězslav Benda (Doc, Ing, PhD) was born in Dvůr Králové n./L., Czech Republic in 1944. He graduated at the Czech Technical University in Prague from solid state physics branch, an obtained the PhD degree in electrotechnology in 1976. During 1967-1973 he was with R&D Department of ČKD Semiconductors. Since 1973 he is teaching at the Czech Technical University in Prague, Faculty of Electrical Engineering, Department of Electrotechnology, since 1983 in a position of Associate Professor. He is a member of the IEE Czech Center Committee from 1994 and its Chairman since 1999. He was a member of many conferences organizing committees (ISPS'92, 94, and '98, ISSE'85, 89, and '95, IEE PEVD'94,PEVD'96, PEVD'98) a Member of International Programme Committee (MIEL'97, IPEMC'97, IPECM'2000, EPE ,IEEE EPE'97, PEMC'98, MIEL'97) and a referee of the Microelectronics & Reliability Journal

Jiří Toušek, (Doc, RNDr, CSc) was born in 1938 in Jindřichův Hradec. He graduated from the Faculty of Mathematics and Physics in Prague in 1961, and works at the Charles University, Faculty of Mathematics and Physics in Department of Macromolecul Physics. He obtained his Associate Professor degree in 1992. His main interests are otoelectric effects and physics of solar cells.